

**NASA TECHNICAL  
MEMORANDUM**



NASA TM X-52174

NASA TM X-52174

FACILITY FORM 602

**N66-17570**

(ACCESSION NUMBER)	(THRU)
<u>16</u>	<u>1</u>
(PAGES)	(CODE)
<u>TMX-52174</u>	<u>33</u>
(NASA CR OR TMX OR AD NUMBER)	(CATEGORY)

**ANALYSIS OF DEVELOPING LAMINAR FLOW AND HEAT TRANSFER  
IN A TUBE FOR A GAS WITH VARIABLE PROPERTIES**

GPO PRICE \$ \_\_\_\_\_

CFSTI PRICE(S) \$ \_\_\_\_\_

by Robert G. Deissler and Alden F. Presler  
Lewis Research Center  
Cleveland, Ohio

Hard copy (HC) 1.00

Microfiche (MF) .50

ff 853 July 65

TECHNICAL PAPER proposed for presentation at Third  
International Heat Transfer Conference  
Chicago, Illinois, August 8-12, 1966

**ANALYSIS OF DEVELOPING LAMINAR FLOW AND HEAT TRANSFER  
IN A TUBE FOR A GAS WITH VARIABLE PROPERTIES**

by **Robert G. Deissler and Alden F. Presler**

**Lewis Research Center  
Cleveland, Ohio**

**TECHNICAL PAPER** proposed for presentation at

**Third International Heat Transfer Conference  
Chicago, Illinois, August 8-12, 1966**

**NATIONAL AERONAUTICS AND SPACE ADMINISTRATION**

**ASME**

# ANALYSIS OF DEVELOPING LAMINAR FLOW AND HEAT TRANSFER IN A TUBE FOR A GAS WITH VARIABLE PROPERTIES

by Robert G. Deissler and Alden F. Presler

Lewis Research Center  
National Aeronautics and Space Administration  
Cleveland, Ohio

## ABSTRACT

Laminar tube flow and heat transfer for helium gas are analyzed numerically by using the compressible Navier-Stokes, energy, and continuity equations in finite difference form. Both radial and axial property variations are considered. The radial as well as the axial velocity are retained in the equations; the only assumptions made in the equations are the usual boundary-layer assumptions. The heat flux at the wall and the initial velocity and temperature profiles are taken to be uniform. The effects of both heat flux and Mach number on the Nusselt number and friction correlations are obtained.

## AUSZUG

Laminarströmung in einer Röhre und Wärmeübertragung für Heliumgas wurden mit Hilfe der kompressiblen Formel von Navier-Stokes und der Energie- und Kontinuitätsformeln in endlicher Differenzform numerisch analysiert. Abweichungen der radialen und axialen Eigenschaften werden in Betracht gezogen. Sowohl die radiale wie die axiale Geschwindigkeit sind in die Gleichungen eingesetzt und nur die üblichen Grenzschichtannahmen sind in den Gleichungen gemacht. Der Wärmestrom an der Wand und die Ausgangsgeschwindigkeit und -temperaturprofile sind als gleichmässig angenommen. Der Einfluss des Wärmestroms und der Machzahl auf die Nusseltzahl und die Reibungsbeziehungen werden erhalten.

## АННОТАЦИЯ

Численным способом для гелия исследуются ламинарный поток в трубке и теплопередача применяя уравнения Навье-Стокса, энергии и неразрывности для сжимаемого газа в виде конечных разностей. Рассматриваются как радиальные так и осевые переменные свойства; в уравнениях сделаны только обычные предположения относительно пограничного слоя. Предполагается равномерность потока тепла на стенке и профилей начальной скорости и температуры. Получены влияния потока тепла и числа Маха на число Нуссельта и на корреляции трения.

## INTRODUCTION

The laminar flow and heat transfer in the entrance regions of passages have been extensively analyzed by a number of workers. The constant-property Graetz problem [1 and 2],<sup>1</sup> in which the velocity profile is assumed fully developed, and where the temperature profile is calculated as a function of distance from the entrance, has been exhaustively explored. Whenever the development of the velocity profile has been considered, integral methods have generally been employed [3], or the nonlinear acceleration terms in the equations of motion have been approximated by linear terms [4 and 5]. A numerical solution for constant-property plane-Poiseuille flow in which the nonlinear terms are retained is given in [6]. Numerical solutions for heat transfer with developing velocity and temperature profiles in a tube are given in [7] and [8]. In those analyses the velocity profiles are obtained from the linearized solution in [4].

For the case of laminar flow with variable fluid properties, only a limited amount of work has been done. An analysis in [9] considers flow in a tube far from the entrance. Radial variations of fluid properties are considered, but axial variations are neglected. The effects of radial velocity are also neglected. In [10] various radial flows are arbitrarily introduced into an analysis in an attempt to study the effects of radial flow on heat transfer and friction with variable prop-

erties. A comparison of the results with the experiments in [10] and [11] indicates that the radial flow could have an important effect. Additional partial solutions, which study effects of variable fluid properties, are given in [12], [13], and [14].

In order to eliminate, as far as possible, the dubious assumptions made in previous analyses, the equations of motion and energy for a gas with variable properties are herein solved numerically. Only the usual boundary-layer assumptions are made. Those assumptions have been made in nearly all of the analyses for flow and heat transfer in tubes, and they generally give good results, except in the region very close to the entrance. The pertinent equations and their solutions for uniform initial velocity and temperature profiles in a tube with uniform wall heating will be considered in the next section.

## ANALYSIS

The equations of motion, energy, and state for a perfect gas, for a steady-state, axially-symmetric flow, without swirl and body forces, can be written as [15]

<sup>1</sup>Numbers in brackets denote references.

$$\rho \left( v_r \frac{\partial v_z}{\partial r} + v_z \frac{\partial v_z}{\partial z} \right) = - \frac{\partial p}{\partial z} + \frac{\partial}{\partial z} \left[ 2\mu \frac{\partial v_z}{\partial z} + \left( \zeta - \frac{2}{3} \mu \right) \left( \frac{1}{r} \frac{\partial}{\partial r} r v_r + \frac{\partial v_z}{\partial z} \right) \right] + \frac{1}{r} \frac{\partial}{\partial r} \left[ \mu r \left( \frac{\partial v_r}{\partial z} + \frac{\partial v_z}{\partial r} \right) \right] \quad (1)$$

$$\rho \left( v_r \frac{\partial v_r}{\partial r} + v_z \frac{\partial v_r}{\partial z} \right) = - \frac{\partial p}{\partial r} + \frac{\partial}{\partial r} \left[ 2\mu \frac{\partial v_r}{\partial r} + \left( \zeta - \frac{2}{3} \mu \right) \left( \frac{1}{r} \frac{\partial}{\partial r} (r v_r) + \frac{\partial v_z}{\partial z} \right) \right] + \frac{\partial}{\partial z} \left[ \mu \left( \frac{\partial v_r}{\partial z} + \frac{\partial v_z}{\partial r} \right) \right] + \frac{2\mu}{r} \left( \frac{\partial v_r}{\partial r} - \frac{v_r}{r} \right) \quad (2)$$

$$\frac{1}{r} \frac{\partial(\rho r v_r)}{\partial r} + \frac{\partial(\rho v_z)}{\partial z} = 0 \quad (3)$$

$$\rho c_p \left( v_r \frac{\partial T}{\partial r} + v_z \frac{\partial T}{\partial z} \right) - v_r \frac{\partial p}{\partial r} - v_z \frac{\partial p}{\partial z} = \frac{1}{r} \frac{\partial}{\partial r} \left( k r \frac{\partial T}{\partial r} \right) + \frac{\partial}{\partial z} \left( k \frac{\partial T}{\partial z} \right) + \mu \left\{ 2 \left[ \left( \frac{\partial v_r}{\partial r} \right)^2 + \left( \frac{v_r}{r} \right)^2 + \left( \frac{\partial v_z}{\partial z} \right)^2 \right] + \left( \frac{\partial v_r}{\partial z} + \frac{\partial v_z}{\partial r} \right)^2 \right\} + \left( \zeta - \frac{2}{3} \mu \right) \left( \frac{\partial v_r}{\partial r} + \frac{v_r}{r} + \frac{\partial v_z}{\partial z} \right)^2 \quad (4)$$

and

$$p = \rho R T \quad (5)$$

If it is assumed that the boundary layer thickness  $\delta \ll z$ , then Equations (1), (2) and (4) reduce to

$$\rho \left( v_r \frac{\partial v_z}{\partial r} + v_z \frac{\partial v_z}{\partial z} \right) = - \frac{\partial p}{\partial z} + \frac{1}{r} \frac{\partial}{\partial r} \left( \mu r \frac{\partial v_z}{\partial r} \right) \quad (6)$$

and

$$\rho c_p \left( v_r \frac{\partial T}{\partial r} + v_z \frac{\partial T}{\partial z} \right) - v_z \frac{\partial p}{\partial z} = \frac{1}{r} \frac{\partial}{\partial r} \left( k r \frac{\partial T}{\partial r} \right) + \mu \left( \frac{\partial v_z}{\partial r} \right)^2 \quad (7)$$

where, from Equation (2),  $p$  and  $\partial p/\partial z$  are essentially independent of  $r$ . The boundary-layer assumption should be valid except, possibly, for the region very close to the entrance.

An expression for the radial velocity  $v_r$  can be obtained by integrating the continuity Equation (3) as follows:

$$v_r = - \frac{1}{\rho r} \int_0^r \xi \left( \rho \frac{\partial v_z}{\partial z} + v_z \frac{\partial \rho}{\partial z} + v_z \frac{\rho_1 T_1}{p_1 T} \frac{\partial \rho}{\partial z} \right) d\xi \quad (8)$$

where the axial density gradient in Equation (3) was eliminated by differentiating the equation of state (Eq. (5)). The subscript 1 refers to values at the tube inlet. The fact that  $v_r = 0$  at the tube axis was used in obtaining Equation (8).

To obtain an expression for the axial pressure gradient, which is independent of  $r$ , Equation (6) at the wall is evaluated:

$$\frac{\partial p}{\partial z} = \frac{1}{r_w} \left[ \frac{\partial}{\partial r} \left( \mu r \frac{\partial v_z}{\partial r} \right) \right]_w \quad (9)$$

By using Equations (5), (6), (7), (8), and (9), the final set of equations to be solved can be written in dimensionless form as

$$\frac{\Delta v_z'}{\Delta z'} \approx \frac{\partial v_z'}{\partial z'} = \frac{1 - q'T'}{r'v_z'(1 - \gamma M_1^2 p')} \frac{\partial v_z'}{\partial r'} \int_0^{r'} \xi \left[ \frac{1 - \gamma M_1^2 p'}{1 - q'T'} \frac{\partial v_z'}{\partial z'} + q' \frac{v_z'(1 - \gamma M_1^2 p')}{(1 - q'T')^2} \frac{\partial T'}{\partial z'} - \gamma M_1^2 \frac{v_z'}{1 - q'T'} \frac{\partial p'}{\partial z'} \right] d\xi + \frac{1 - q'T'}{v_z'(1 - \gamma M_1^2 p')} \frac{\partial p'}{\partial z'} + \frac{2(1 - q'T')}{Re_1(1 - \gamma M_1^2 p')v_z'r'} \left( \mu'r' \frac{\partial^2 v_z'}{\partial r'^2} + \mu' \frac{\partial v_z'}{\partial r'} + r' \frac{\partial \mu'}{\partial r'} \frac{\partial v_z'}{\partial r'} \right) \quad (10)$$

$$\frac{\Delta T'}{\Delta z'} \approx \frac{\partial T'}{\partial z'} = \frac{1 - q'T'}{(1 - \gamma M_1^2 p')r'v_z'} \frac{\partial T'}{\partial r'} \int_0^{r'} \xi \left[ \frac{(1 - \gamma M_1^2 p')}{1 - q'T'} \frac{\partial v_z'}{\partial z'} + \frac{q'v_z'(1 - \gamma M_1^2 p')}{(1 - q'T')^2} \frac{\partial T'}{\partial z'} - \gamma M_1^2 \frac{v_z'}{1 - q'T'} \frac{\partial p'}{\partial z'} \right] d\xi + \frac{(\gamma - 1)M_1^2(1 - q'T')}{q'c_p'(1 - \gamma M_1^2 p')} \frac{\partial p'}{\partial z'} + \frac{2}{Re_1 Pr_1} \frac{1 - q'T'}{(1 - \gamma M_1^2 p')c_p'v_z'r'} \left( k'r' \frac{\partial^2 T'}{\partial r'^2} + k' \frac{\partial T'}{\partial r'} + r' \frac{\partial k'}{\partial r'} \frac{\partial T'}{\partial r'} \right) - \frac{2(\gamma - 1)M_1^2}{q'Re_1 c_p'} \frac{\mu'(1 - q'T')}{(1 - \gamma M_1^2 p')v_z'} \left( \frac{\partial v_z'}{\partial r'} \right)^2 \quad (11)$$

$$\frac{\Delta p'}{\Delta z'} \approx \frac{\partial p'}{\partial z'} = -\frac{2}{Re_1} \left( \mu' r' \frac{\partial^2 v_z'}{\partial r'^2} + \mu' \frac{\partial v_z'}{\partial r'} + r' \frac{\partial \mu'}{\partial r'} \frac{\partial v_z'}{\partial r'} \right) \quad (12)$$

In order to compare results with those in [9], the following values are used:

$$\mu' = k' = \left( \frac{T'}{T_1} \right)^{0.68} = (1 - q'T')^{0.68} \quad (13)$$

$$c'_p = 1, \quad (14a)$$

and

$$Pr_1 = 0.667 \quad (14b)$$

These properties also correspond closely to those for helium, so that these results should apply to that gas.

To carry out the numerical solution the derivatives in Equations (10), (11), and (12) are replaced by their finite difference forms. For instance,  $\partial v_z'/\partial r'$  is replaced by  $(v'_{z,r+\Delta r} - v'_{z,r-\Delta r})/2\Delta r'$ , and  $\partial^2 v_z'/\partial r'^2$  by  $(v'_{z,r+\Delta r} - 2v'_{z,r} + v'_{z,r-\Delta r})/(\Delta r')^2$ . In the problem considered here, the velocity and temperature profiles are uniform at the tube inlet, and the heat flux at the tube wall is also uniform. Thus, the initial conditions can be written in dimensionless form as follows: At the tube inlet ( $z' = 0$ ),  $T' = 0$ ,  $p' = 0$ , and  $v_z' = 1$  (except at  $r' = 1$ , where  $v_z' = 0$ ). For the boundary conditions at the wall ( $r' = 1$ ),  $v_z' = 0$  and

$\partial T'/\partial r' = -1/k'$ . At the tube axis ( $r' = 0$ ),  $\partial v_z'/\partial r' = 0$  and  $\partial T'/\partial r' = 0$ . Since the wall heat flux is uniform, the parameter  $q'$  is set equal to a constant for each numerical run.

With the foregoing initial and boundary conditions, Equations (10), (11), (12), (13), and (14) can be used in finite difference form to calculate  $v_z'$ ,  $T'$ , and  $p'$  at various increments of  $z'$ . The values of  $\partial v_z'/\partial z'$  and  $\partial T'/\partial z'$  occurring on the right sides of the equations are generally not known at  $z' = 0$ , but they may be found by iteration by assuming values for them and then calculating new values from the equations. For later  $\Delta z$  steps, values of  $\partial v_z'/\partial z'$  and  $\partial T'/\partial z'$  from the preceding step can be substituted in the right sides of the equations. These might again be iterated, although it may not be necessary for sufficiently small values of  $\Delta z$ . The calculations can also be carried out by a matrix method which avoids the use of iteration. In the calculations, the ratio of  $\Delta z'$  to  $(\Delta r')^2$  must be kept sufficiently small to ensure stability of the solution. The quantity  $\Delta r'$  must also be made small enough so that cutting it in half does not change the results appreciably. The calculations were carried out on a high speed digital computing machine. With the dimensionless velocity and temperature profiles, as well as the pressure, calculated as functions of  $z'$ ,  $R$ ,  $M_1$ , and  $q'$ , the following integral quantities can be obtained:

$$v'_{z,b} = 2 \int_0^1 v_z' r' dr' \quad (15)$$

$$T'_b = \frac{\int_0^1 T' \frac{v_z' r'}{1 - q'T'} dr'}{\int_0^1 \frac{v_z' r'}{1 - q'T'} dr'} \quad (16)$$

$$T'_{t,b} = \frac{\int_0^1 T'_t \frac{v_z' r'}{1 - q'T'} dr'}{\int_0^1 \frac{v_z' r'}{1 - q'T'} dr'} \quad (17)$$

where

$$T'_t = T' - \frac{\gamma - 1}{2} \frac{M_1^2}{q'} v_z'^2 \quad (18)$$

$$Re_b = \frac{\rho_b' v_{z,b}' Re_1}{\mu'_b} = \frac{(1 - \gamma M_1^2 p') v_{z,b}' Re_1}{(1 - q'T'_b)(1 - q'T'_b)^{0.68}} \quad (19)$$

$$Nu_b = \frac{2}{k'_b (T'_{t,b} - T'_{t,w})} = \frac{2}{(1 - q'T'_b)^{0.68} (T'_{t,b} - T'_{t,w})} \quad (20)$$

$$f'_{\tau,b} = \frac{4(1 - q'T'_b) \tau'}{(1 - \gamma M_1^2 p') v_{z,b}'^2 Re_1} \quad (21)$$

where

$$\tau' = \mu'_w \left( \frac{\partial v_z'}{\partial r'} \right)_w = (1 - q'T'_w)^{0.68} \left( \frac{\partial v_z'}{\partial r'} \right)_w \quad (22)$$

$$\delta_b = \frac{\tau'}{v_{z,b}' \mu'_b} = \frac{\tau'}{v_{z,b}' (1 - q'T'_b)^{0.68}} \quad (23)$$

$$f'_{\epsilon,b} = \frac{dp'/dz'}{2\rho_b' v_{z,b}'^2} = \frac{(1 - q'T'_b) dp'/dz'}{2(1 - \gamma M_1^2 p') v_{z,b}'^2} \quad (24)$$

$$f'_{p,b} = \frac{p'}{2z' \rho_b' v_{z,b}'^2} \quad (25)$$

Results calculated from these equations will be given in the next section.

## RESULTS AND DISCUSSION

Friction factor curves are presented in Figures 1, 2, and 3, and corresponding Nusselt number results for heat transfer are given in Figure 4. Friction factors based on wall shear stress, pressure gradient, and pressure drop are shown. They are multiplied by  $Re_b$ , since friction factor times  $Re_b$  is not a function of  $Re_b$  but is a function only of  $(z/D)/Re_b$ ,  $q'$ ,  $M_1$ , and  $Pr_1$ . The Nusselt number  $Nu_b$  is also a function only of those variables. In the uniform property case, friction parameters and Nusselt numbers approach constant values for large distances from the entrance.

In Figures 1 to 3, the calculated friction factor curves for uniform properties ( $q' = M_1 = 0$ ) are compared with the linearized

analyses from [4] and [5], and with the experimental data from [16]. These calculated curves are in substantial agreement with the data and the linearized analyses, except for the linearized results for shear stress shown in Figure 1. The latter apparently deviate because the shear stress is very sensitive to the effect of the linearizing approximation.

In Figure 4, the calculated Nusselt number curves for uniform properties are compared with the analysis from [8]. The main difference between the present analysis and that in [8] is that the latter is based on the linearized velocity profiles from [4], whereas the present analysis does not use a linearizing approximation. The comparison shows that the effect of the linearizing approximation on the Nusselt number plot is small. Results from [8] for  $v_r = 0$  (not shown) are also in good agreement with those calculated here, although the original calculations for  $v_r = 0$  from [7] showed somewhat more deviation because of the larger increment size used there.

Curves for moderately high heat transfer to the gas ( $q' = 13.5$ ) and for  $M_1 = 0$  and  $M_1 = 0.06$  are also shown in Figures 1 to 4. For the runs shown, the maximum temperature ratio  $T_w/T_b$  occurs in the entrance region and is about 2.7. At the point where  $Nu_b$  is a minimum,  $T_w/T_b$  is about 1.5. The effect of the heat flux on the friction factor is much greater than that on the Nusselt number. Values of the friction parameters are, in general, increased considerably by the heat transfer to the gas. On the other hand, the Nusselt numbers in the entrance region are increased but slightly, and part of that increase may be due to the slightly lower Prandtl number used for the runs in which  $q' > 0$ . The fact that the effect of variable properties on the bulk Nusselt number correlation is small in the entrance region is in agreement with the experimental finding in [11]. Farther down the tube the values of Nusselt number dip below the fully developed value for uniform properties. Finally, still farther down the tube, the Nusselt numbers for  $q' > 0$  and  $M_1 = 0$  again approach the uniform property value of 48/11. This happens inasmuch as the absolute temperature ratio  $T_w/T_b$  approaches 1 because of the increase in temperature level along the tube, even though the heat flux is uniform. Thus, radially uniform fluid properties are approached far down the tube, although the properties still vary axially. The values of  $f_{\tau,b} Re_b$  also approach the fully developed uniform property value at large values of  $(z/D)/Re_b$ . Therefore, the axial variation of properties does not seem to affect the values of  $Nu_b$  and of  $f_{\tau,b} Re_b$  in the region far from the entrance. The behavior of  $f_{g,b} Re_b$  and  $f_{p,b} Re_b$  at large distances from the entrance is more complicated because those quantities include pressure changes due to momentum effects.

For  $M_1 > 0$  and  $q' > 0$  both the Nusselt numbers (Fig. 4) and shear-stress friction factors (Fig. 1) increase rapidly near the end of the run. This occurs because the local Mach number approaches 1 and choking takes place. These large increases in Nusselt number and shear stress are evidently associated with the large accelerations that occur near a Mach number of 1.

Numerical calculations of Nusselt number, such as those given in Figure 4, might be used in conjunction with measurements of heat-transfer coefficients in tubes to obtain the thermal con-

ductivities of gases at high temperatures. The use of such calculations would allow measurements at reasonably high heat fluxes, so that greater accuracy could be obtained than would be possible if it were necessary to keep the heat fluxes small enough to approximate uniform properties. An advantage of this method of obtaining thermal conductivities at high temperatures is that radiation effects are small.

Velocity profiles which correspond to the curves in Figures 1 to 4 for  $M_1 = 0.06$  and  $q' = 13.5$  are plotted in Figure 5. At  $z = 0$  the profile is, of course, flat by assumption. As  $z$  increases, the fluid near the wall accelerates because of the heat addition. This causes a peak in the curve to develop away from the tube axis. Farther down the tube the profile tends to approach a fully developed parabolic shape. Then, as a Mach number of 1 is approached, the profile flattens because of the acceleration of the fluid near the wall. This region of flattening corresponds to the region of rising values of  $f_{\tau,b} Re_b$  and  $Nu_b$  in Figures 1 and 4.

Figures 6 and 7 compare the present zero Mach number results for the quasi-developed region with those in [9], where the effect of radial variation of properties is considered, but axial effects and radial flow are neglected. Values of  $Nu_b$  and of the friction parameter  $\delta_b = f_{\tau,b} Re_b$  are plotted against temperature ratio  $T_w/T_b$  for heat addition to the gas. The region of quasi-developed flow for the present results was somewhat arbitrarily taken as the region beyond the minimum in the Nusselt number curves.

The Nusselt number results from [9] are in reasonably good agreement with the present results, which decrease slowly with increasing values of  $T_w/T_b$ . In the case of the friction parameter, although both the present results and those from [9] show an increase in  $\delta_b$  with increasing  $T_w/T_b$ , the increases shown by the present analysis are considerably greater. Experimental data from [10] also showed increases in friction considerably greater than those predicted in [9]. The conclusion to be drawn, then, is that axial changes and radial flow are not important as far as the quasi-developed heat-transfer correlation is concerned, but that those factors can have a considerable effect on the friction.

#### SUMMARY OF RESULTS

The calculated heat-transfer and pressure-drop results for uniform properties agreed reasonably well with analyses which make use of linearizing approximations in the momentum equation. Linearized shear-stress results, however, showed deviation from the present calculations, apparently because the shear stress is very sensitive to the effect of the linearizing approximation. Calculated pressure-gradient and pressure-drop results for uniform properties were in satisfactory agreement with available experimental data.

The variable-property friction-factor curves with properties evaluated at the fluid bulk temperature showed that the level of the curves can be increased considerably by heat transfer to the gas. On the other hand, the Nusselt number correlation based on the bulk temperature was affected but slightly by variable properties in the entrance region. Farther down the tube, the Nusselt numbers with large heat transfer to the gas dropped below the fully developed uniform property value. However, when the Mach number approached 1 near the

end of the tube, both the Nusselt number and the friction parameter increased sharply.

The numerical method used here for calculating Nusselt numbers in variable-property streams may be useful in obtaining thermal conductivities of gases at high temperatures by measurement of heat-transfer coefficients.

The results calculated here for the quasi-developed region and a Mach number of zero were compared with those from a previous analysis (NACA TN-2410) which considered the radial variation of properties but neglected axial effects and radial flow. The comparison showed that axial effects and radial flow have but a slight effect on the heat transfer results, but they have a marked effect on the shear stress.

SYMBOLS

D	tube diameter
$c_p$	specific heat at constant pressure
$c_p^i$	$c_p/c_{p,i}$
$c_v$	specific heat at constant volume
$f_{\tau,b}$	$2\tau_w/(\rho_b v_{z,b}^2)$ friction factor based on wall shear stress with density evaluated at $T_b$
$f_{g,b}$	$-\frac{1}{2}[dp/d(z/D)]/(\rho_b v_{z,b}^2)$ friction factor based on pressure gradient with density evaluated at $T_b$
$f_{p,b}$	$(1/2)(p_i - p)/[(z/D)\rho_b v_{z,b}^2]$ friction factor based on pressure drop with density evaluated at $T_b$
h	$q/(T_{t,w} - T_{t,b})$ , heat transfer coefficient
k	thermal conductivity of gas
$k'$	$k/k_i$
$M_i$	$v_{z,i}/\sqrt{\gamma RT_i}$
$Nu_b$	$hD/k_b$ Nusselt number with conductivity evaluated at $T_b$
p	pressure
$p'$	$(p_i - p)/(\rho_i v_{z,i}^2)$
$Pr_i$	$c_{p,i}\mu_i/k_i$ Prandtl number at inlet
q	heat transfer per unit area from wall to fluid
$q'$	$qr_w/(T_i k_i)$
r	distance from tube axis
$r_w$	tube radius
$r'$	$r/r_w$
$Re_i$	$\rho_i v_{z,i} D/\mu_i$ inlet Reynolds number
R	perfect gas constant
$Re_b$	$\rho_b v_{z,b} D/\mu_b$ local bulk Reynolds number
T	absolute temperature
$T'$	$(T_i - T)k_i/(qr_w)$
$T_b$	bulk temperature
$T_b^i$	$(T_i - T_b)k_i/(qr_w)$ , Equation (16)
$T_t$	absolute total temperature
$T_t^i$	$(T_i - T_t)k_i/(qr_w)$
$T_{t,b}$	bulk total temperature
$T_{t,b}^i$	$(T_i - T_{t,b})k_i/(qr_w)$ , Equation (17)
$v_r$	radial velocity
$v_z$	axial velocity
$v_z^i$	$v_z/v_{z,i}$
z	axial distance from tube inlet
$z'$	$z/r_w$
$\gamma$	$c_p/c_v$

$\delta_b$	$\tau_w/(v_{z,b}\mu_b)$ , shear stress parameter, Equation (23)
$\xi$	second viscosity coefficient ( $\xi = 0$ for monatomic gas)
$\mu$	viscosity
$\mu'$	$\mu/\mu_i$
$\rho$	density
$\rho'$	$\rho/\rho_i$
$\tau$	wall shear stress
$\tau'$	$\tau_w/(v_{z,i}\mu_i)$

Subscripts:

b	bulk, evaluated at bulk or mixed mean temperature
i	at tube inlet
w	at wall

Superscripts:

'	on dimensionless quantity
---	---------------------------

REFERENCES

- Sellars, J. R., M. Tribus, and J. S. Klein, "Heat Transfer to Laminar Flow in a Round Tube or Flat Conduit - The Graetz Problem Extended," ASME Trans., vol. 78, no. 2, February, 1956, pp. 441-448.
- Siegel, R., E. M. Sparrow, and T. M. Hallman, "Steady Laminar Heat Transfer in a Circular Tube with Prescribed Wall Heat Flux," Appl. Sci. Res., Sec. A, vol. 7, 1958, pp. 386-392.
- Schiller, L., "Die Entwicklung der Laminaren Geschwindigkeitverteilung und ihre Bedeutung für Zähigkeitmessungen," Z. Angew. Math. Mech., vol. 2, 1922, pp. 96-106.
- Langhaar, H. L., "Steady Flow in the Transition Length of a Straight Tube," J. Appl. Mech., vol. 9, no. 2, June, 1942, pp. 55-58.
- Sparrow, E. M., S. H. Lin, and T. S. Lundgren, "Flow Development in the Hydrodynamic Entrance Region of Tubes and Ducts," Phys. Fluids, vol. 7, no. 3, March, 1964, pp. 338-347.
- Bodoia, J. R., and J. F. Osterle, "Finite Difference Analysis of Plane Poiseuille and Couette Flow Developments," Appl. Sci. Res., Sec. A, vol. 10, no. 3-4, 1961, pp. 265-276.
- Kays, W. M., "Numerical Solutions for Laminar-Flow Heat Transfer in Circular Tubes," ASME Trans., vol. 77, no. 11, November, 1955, pp. 1265-1274.
- Ulrichson, D. L. and R. A. Schmitz, "Laminar-Flow Heat Transfer in the Entrance Region of Circular Tubes," Int. J. Heat Mass Transfer, vol. 8, no. 2, February, 1965, pp. 253-258.
- Deissler, R. G., "Analytical Investigation of Fully Developed Laminar Flow in Tubes with Heat Transfer with Fluid Properties Variable Along the Radius," NACA TN 2410, July, 1951.
- Davenport, M. E. and G. Leppert, "The Effect of Transverse Temperature Gradients on the Heat Transfer and Friction for Laminar Flow of Gases," J. Heat Transfer, vol. 87, no. 2, May, 1965, pp. 191-196.
- Kays, W. M. and W. B. Nicoll, "Laminar Flow Heat Transfer to a Gas with Large Temperature Differences," J. Heat Transfer, vol. 85, no. 4, November, 1963, pp. 329-338.

12. Koppel, L. B. and J. M. Smith, "Laminar Flow Heat Transfer for Variable Physical Properties," *J. Heat Transfer*, vol. 84, no. 2, May, 1962, pp. 157-163.
13. Pigford, R. L., "Nonisothermal Flow and Heat Transfer Inside Vertical Tubes," *Chem. Eng. Progr. Symposium Ser.*, vol. 51, no. 17, 1955, pp. 79-92.
14. Hanratty, T. J., E. M. Rosen, and R. L. Kabel, "Effect of Heat Transfer on Flow Field at Low Reynolds Numbers in Vertical Tubes," *Ind. Eng. Chem.*, vol. 50, no. 5, May, 1958, pp. 815-820.
15. Hughes, W. F. and E. W. Gaylord, *Basic Equations of Engineering Science*, Schaum Publishing Co., New York, 1964, pp. 15, 36, 37.
16. Shapiro, A. H., R. Siegel, and S. J. Kline, "Friction Factor in the Laminar Entry Region of a Smooth Tube," *Proceedings of the Second U. S. National Congress of Applied Mechanics*, P. M. Naghdi, ed., ASME, 1955, pp. 733-741.

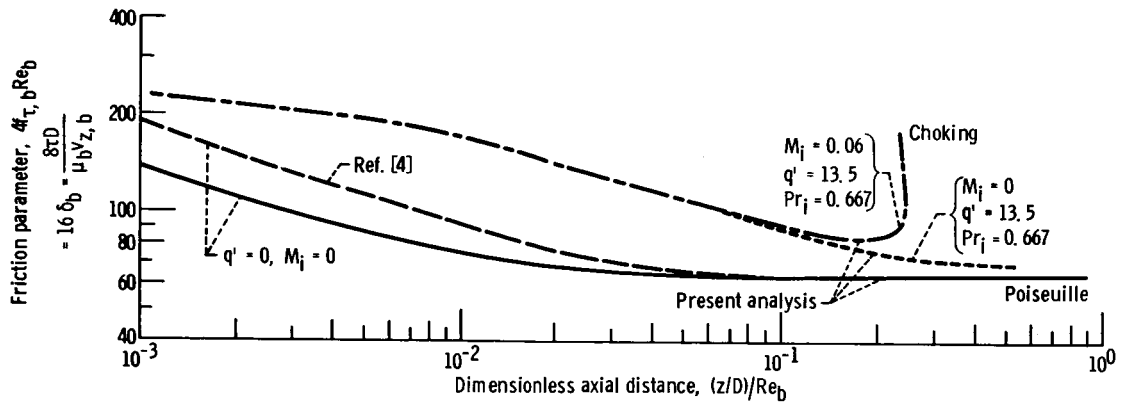


Fig. 1. - Friction parameter based on local wall shear stress plotted against dimensionless distance from tube entrance.

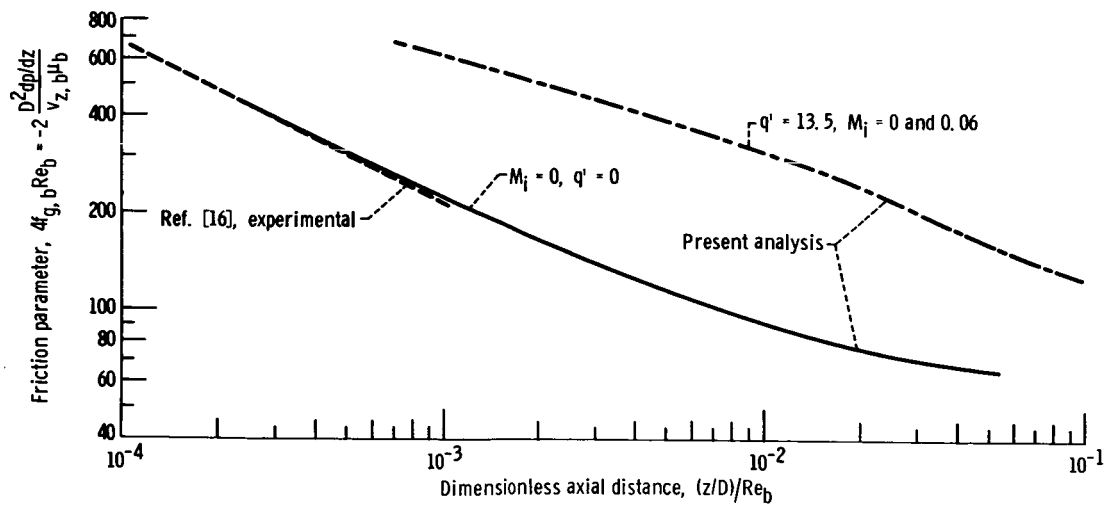


Fig. 2. - Friction parameter based on local pressure gradient plotted against dimensionless distance from tube entrance.

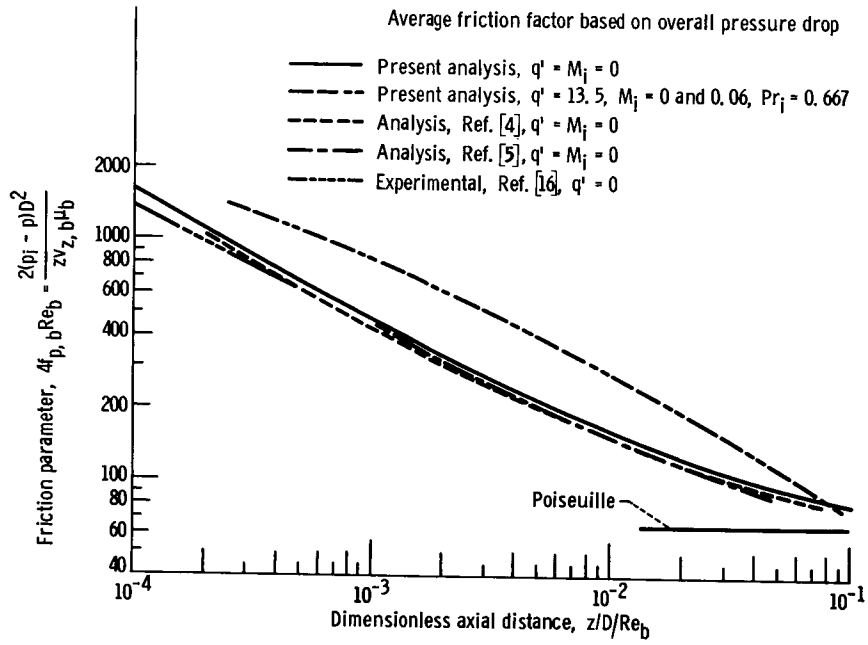


Fig. 3 - Friction parameter based on pressure drop plotted against dimensionless distance from tube entrance.

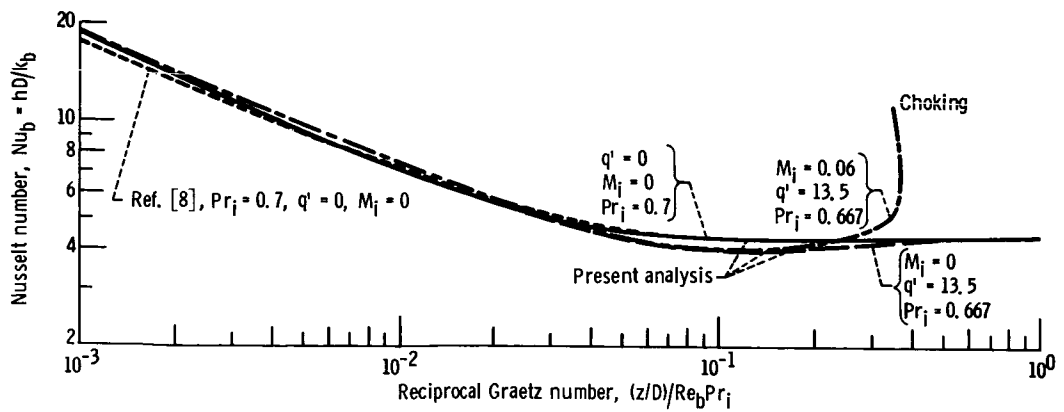


Fig. 4 - Local Nusselt number plotted against dimensionless distance from tube entrance.

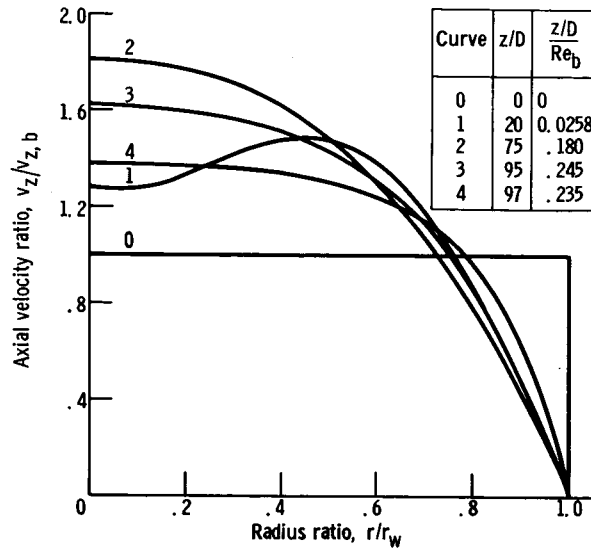


Fig. 5. - Curves showing development of velocity profile.  $q' = 13.5$ ;  $M_1 = 0.06$ ;  $Pr_1 = 0.667$ . (Values of  $z/D$  are for  $Re_1 = 1500$ .)

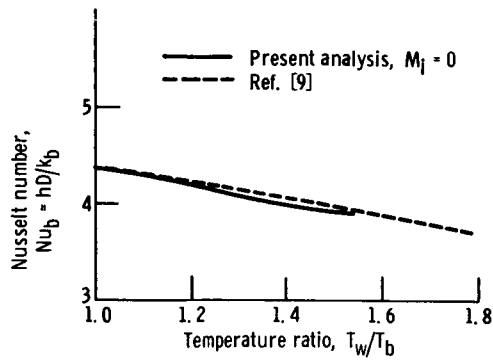


Fig. 6. - Effect of temperature ratio on Nusselt number for quasi-developed flow ( $M_1 = 0$ ).

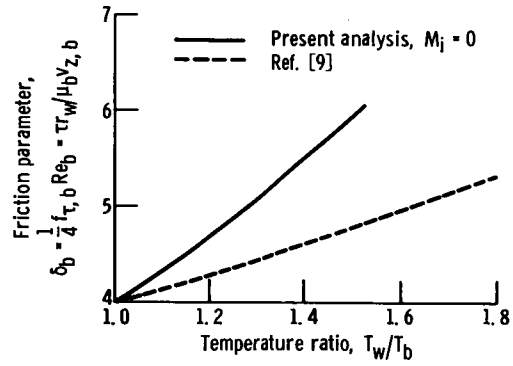


Fig. 7. - Effect of temperature ratio on friction parameter for quasi-developed flows ( $M_i = 0$ ).